Chapter 9

Adaptive Management Framework for Evaluating and Adjusting Microclimate Parameters in Tropical Greenhouse Crop Production Systems

Redmond R. Shamshiri, Muhammad Razif Mahadi,
Kelly R. Thorp, Wan Ishak Wan Ismail,
Desa Ahmad and Hasfalina Che Man

Additional information is available at the end of the chapter

http://dx.doi.org/10.5772/intechopen.69972

Abstract

High operational costs of greenhouse production in hot and humid climate condition due to the initial investments on structure, equipment, and energy necessitate practicing advanced techniques for more efficient use of available resources. This chapter describes design and concepts of an adaptive management framework for evaluating and adjusting optimality degrees and comfort ratios of microclimate parameters, as well as predicting the expected yield in greenhouse cultivation of tomato. A systematic approach is presented for automatic data collection and processing with the objective to produce knowledge-based information in achieving optimum microclimate for high-quality and high-yield tomato. Applications of relevant computer models are demonstrated through case-study examples for use in an iterative way to simulate and compare different scenarios. The presented framework can contribute to future studies for providing best management decisions such as site selection, optimum growing season, scheduling efficiencies, energy management with different climate control systems, and risk assessments associated with each task.

Keywords: greenhouse, climate control, microclimate evaluation, tomato, ventilation, evaporative cooling

1. Introduction

The increasing market demand for high-quality food products have replaced open-field cultivations of Solanaceae and Cucurbits crops with modern plant production systems for more efficient use of available resources. Closed-field cultivations by means of commercial

greenhouses have been changed over the last three decades from basic structures to advanced controlled environments for optimizing plant's productivity and producing high yields at low expenses. The higher costs of greenhouse operation due to the initial investments on structure, equipment, and energy necessitate practicing advanced techniques of automation for efficient control of the microenvironment. Research trends in this field are directed toward developing innovative solutions for shifting from energy-consuming to energy neutral greenhouses with the ultimate objective of increasing profits. This is, however, challenging due to the lack of accurate information about interactions between crops and environment at different growth stages, as well as the complexity of the dynamic system that is subjected to changes with internal and external factors. Plant-based engineering has helped researchers with proper management policies to embrace these uncertainties through modeling and integrated-learning approaches. Several uncertainties with greenhouse cultivation include climate variability, expected yield, optimum references of microclimate parameters, comfort ratios, insecurity of resources, complexity of the system states, lack of accurate information about interactions between plants and environment, and the relationships between biological and ecological system.

Greenhouse microclimate control has been a large field of study for many years. Much work has been done for moderate cold climate conditions as opposed to tropical lowlands. In contrast to cold arid climate, the main objective of a greenhouse in hot and humid regions such as lowlands of south-east Asia (**Figure 1**) is to protect crop against fluctuations of external conditions such as extreme winds, heavy seasonal rainfalls, typhoons, extreme solar radiation, occasional water shortage, high air temperature, high humidity, and invasion of pests and diseases. The major concern with greenhouses in these regions is the crop stress due to the adverse microclimate that reduces plant evapotranspiration rate and causes production failure. Evaporative cooling systems by means of misting, pad-and-fan, and swamp cooling are widely used in tropical greenhouses of south-east Asia for manipulating crop growth microclimate; however, these systems have not reached their optimum potential due to their conventional automation and control methods. If properly managed, tropical greenhouses can provide suitable growth condition for tomato cultivation by maintaining inside microclimate close to the outside, with an expected yield that varies between 30 and over 100 tons/ha (vs. open-field yield of 15–30 tons/ha) depending on soil culture or hydroponics medium.

Profitability and investment returns of commercial greenhouses are tightly linked to management decisions. One of the main factors to be considered in this context is the sustainability of

Figure 1. Outside and inside view of tropical greenhouses in the lowlands of Malaysia.

http://dx.doi.org/10.5772/intechopen.69972

operations through proper management of available resources. Modern greenhouses are required to exhibit integration of automation, cultural practices, and environmental control using object-oriented analysis of the subsystems. The primary concepts and methods of automation-culture-environment system analysis (ACESYS) in controlled environments plant production (CEPP) have been introduced and expanded in the works of [1–3]. Some of the earliest examples of object-oriented analysis and modeling applications including optimal control strategies and decision-support software in advanced CEPP systems can be found in the works of [2, 4–6]. The purpose of object-oriented system analysis approach according to Ref. [3] is to develop a set of foundation classes that can be used to effectively describe the components of the automation system. This, however, requires a comprehensive understanding of the interaction between crop's growth response and environment characteristics. Some of the specific applications and benefits of system analysis in greenhouse production includes integrated energy-efficient strategies, extracting unique and new knowledge that provides valuable insight to local growers and beyond, understanding limitations of resources and balancing between input and output expectancies, improving technology and increasing returns, providing business attraction for local stakeholders, minimizing energy requirements and eliminating tedious operations, increasing production quality and quantity to satisfy market demands, and technology adaptation by balancing between fixed and flexible automation for various crop production. With this perspective, the convolution of several possible scenarios and combination of culture classes (i.e., climate control parameters) and objects (i.e., tomato crop at different growth stages) necessitates computer-based analysis program within the concepts of a systematic framework approach such as adaptive management.

Adaptive management was initially introduced at the University of Florida [7] as an iterative method for managing natural resource in the systems with wide range of responses to management choices and to help manager's difficulty in understanding the systems' dynamics [8] and plant's responses [9]. It is defined as "a systematic process for continually improving management policies and practices by learning from the outcomes of operational programs" [10]. Adaptive management was created based on the needs of environment and ecosystem managers with an iterative processing tool that acknowledged complexity and uncertainty, with a focus on learning and for continuous inputs [11]. It has been widely used as a new design technique for large database that manages and assists the immense data collection, data analysis, and data storage of distributed sets of experiments associated with environmental, meteorological, biological, and medical research problems or other technical and experimental assessments that utilize large-scale data sources within multiple and separate engineering or laboratory facilities. Examples include the work of Refs. [12–15]. The principles of adaptive management according to Ref. [16] suggest using the best available knowledge to design and implement management plans, while establishing an institutional structure that enables learning from outcomes to adjust and improve future decision making. This structured approach is an efficient method in developing decision-support tools for systems design, management, and operation by recognizing the importance of natural variability in contributing to ecological resilience and productivity.

This chapter provides a systematic process of incorporating new and existing knowledge that can be used in developing management decisions for achieving optimum microclimate.

It describes design and concepts of an adaptive management framework for evaluating optimality degrees and comfort ratios of air temperature (T), relative humidity (RH), and vapor pressure deficit (VPD), as well as prediction of the expected yield in greenhouse cultivation of tomato. The presented framework was designed to allow production managers to ask "what-if" type of questions for further quantitative inclusion to avoid possible detriment decisions. It also provides an in-depth rigorous analysis tool for decision making or decision procrastination when facing uncertainties. It can assist in enhancing scheduling efficiency and guiding investments through different simulated scenarios that are based on information analysis to support optimal restoration strategies. In the rest of this chapter, we refer to the term "microclimate parameters T, RH, or VPD" by $\mathcal{M}$. We also use $Opt(\mathcal{M}) = \alpha$, and $Cft(\mathcal{M}, t, \alpha) = \beta$, to refer to the terms "optimality degree" and "comfort ratio," respectively, defined in Sections 3.1 and 3.2.

2. Adaptive greenhouse model

The key to an adaptive greenhouse is the computer model that drives specific implementations of other components. An adaptive management framework for microclimate evaluation and control in greenhouse production systems is proposed in **Figure 2**. A diagram of the steps in the analysis process is shown by rectangles. The arrows are the direction of the process, and the central spiral highlights the goal of arriving at a compromising decision based on a shared set of objectives developed through the iterative process. The three essential elements in this structure are (i) data entry and retrieval, (ii) computer model (expressed by mathematical equations), and (iii) data

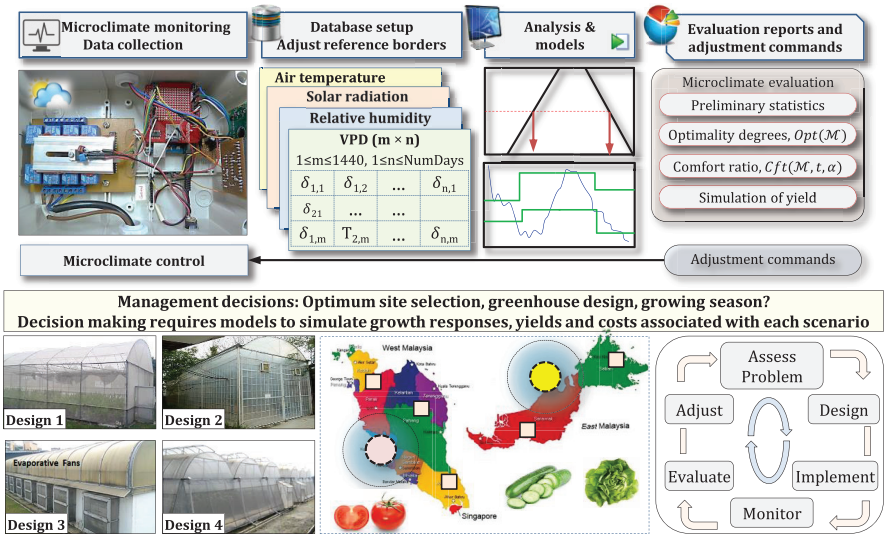

Figure 2. Diagram of the adaptive management framework for monitoring, data processing, evaluating, and adjusting greenhouse microclimate with an iterative analysis approach for scenario analysis with greenhouse crop production.

http://dx.doi.org/10.5772/intechopen.69972

analysis components. The data entry component may be implemented by direct interfacing with real-time data acquisition system or by using web-based and desktop application software. Computer model is application specific; it can be updated and is usually condensed and produced from previous extensive research works in crop physiology. Data analysis comprises implementing relevant techniques within the retrieval component (i.e., programmable spread sheets) or by integrating with third-party applications (i.e., Simulink blocks). The proposed framework can be adapted to new research projects for working with different culture classes and objects by which many specific scenarios may be modeled and analyzed. It carefully monitors the possible outcomes of the system for better understanding of the process in order to adjust control parameters through an iterative learning process.

The framework utilizes a custom-designed data acquisition, and control system [17] that was built using Arduino Uno prototype microcontroller board for monitoring and manipulating of the microclimate parameters. Three computer models were employed by the framework for evaluation and adjusting of optimality degrees $Opt(\mathcal{M})$, comfort ratio $Cft(\mathcal{M}, t, \alpha)$, and prediction of the expected yield. The framework was implemented in MATLAB® (The MathWorks Inc, Natick, MA, USA) environment through Simulink blocks and coding of various main functions and sub-functions that were stored as "m-files." Different toolboxes were developed for the immense data-analyzing tasks as shown in **Figure 3**. The framework structure was designed in a way that end users can create (or update) entries in database, select report type (1-day or multidays report), and proceed with a specific analysis procedure. The database is a dynamic flat file type that can be created by entering collected data, either manually from previously stored sources such as excel sheets or directly from the hardware interface. The computer models presented in this chapter are focused on tomato (*Lycopersicon*

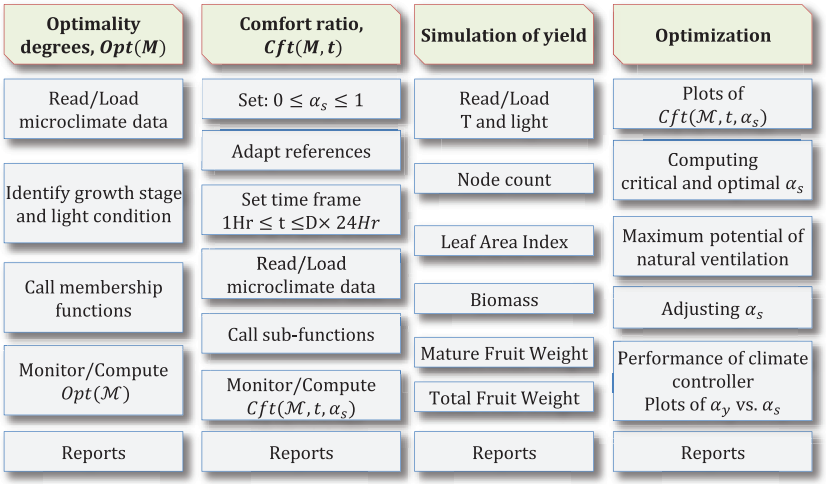

Figure 3. Arrangement of the process in the framework toolboxes.

esculentum); however, with slight modification, the framework can be reprogrammed to work with other greenhouse crops provided that their yield prediction and growth response models are available. Results of microclimate evaluation and set-point manipulation discussed in Sections 3 and 4 can contribute to dynamic greenhouse climate control strategies [18] such as the one in Ref. [19]. An example is provided by comparing a model reference-adaptive greenhouse microclimate controller with conventional closed-loop feedback shown in **Figure 4**. In this scheme, the control law is adapted with the new greenhouse states based on the optimized set points as shown in the diagram of **Figure 5** [19] for a specific microclimate

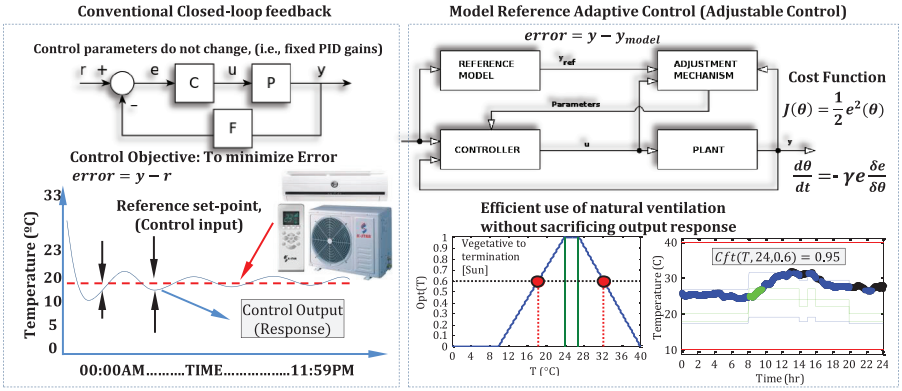

Figure 4. Demonstration of conventional greenhouse controller (left) versus model reference adaptive controller (right).

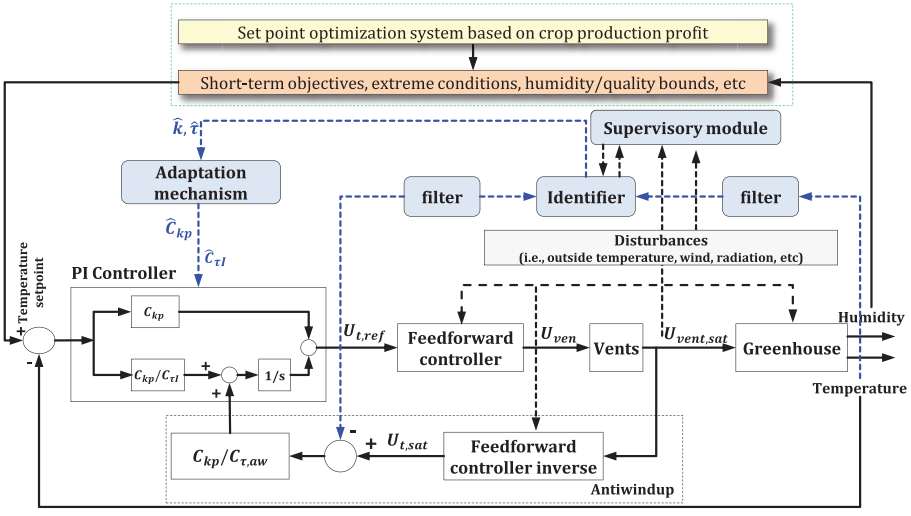

Figure 5. Adaptive control of greenhouse air temperature based on manipulated set point as discussed in Ref. [19].

http://dx.doi.org/10.5772/intechopen.69972

parameter (i.e., air temperature), causing other microclimate parameter (i.e., humidity) to be actually controlled via set-point manipulation.

3. Microclimate evaluation with manipulated set points

3.1. Optimality degrees of microclimate

Optimality degree of a microclimate parameter denoted by $Opt(\mathcal{M}) = \alpha$ is a quantitative value between 0 and 1 that represents how close a microclimate measurement (T, RH, or VPD) is to its ideal value as required by the greenhouse crop at specific growth stage and climate condition. This value can be computed from experimental models that correlate different levels of microclimate parameters with yield and quality of the greenhouse crop. An example of such models is the one developed for air temperature and relative humidity by the Ohio Agricultural Research and Development Center [20, 21]. These models define optimality degrees of *T*, *RH* for greenhouse cultivation of tomato with independent trapezoid membership-function growth response plots that are specific for different growth stages and three light conditions (night, sun, and cloud). These plots were originated using utility theory with the goal of simultaneously achieving high-yield and high-quality fruit. The knowledge behind these plots was condensed from extensive scientific literature and peer-reviewed published research on greenhouse tomato production and physiology. Mathematical expressions and plots of membership functions for defining optimality degrees of T and RH are available in Ref. [22]. The sets of membership functions for defining optimality degrees of VPD are presented in the work of Ref. [23]. According to this model, a membership function for specific growth stage and light condition on the universe of discourse is defined as $Opt(\mathcal{M})_{GS,\ (Light)} : \mathcal{M} \rightarrow [0, 1]$, where $\mathcal{M}: T, RH, and\ VPD$ is the universe of discourse (input). In other words, each $\mathcal{M}$ reading in the greenhouse at time $t_{m,n}$, is mapped to a value between 0 and 1 that quantifies its optimality for tomato production. The two indexes *m* and *n* refer to specific minute and date of a measurement. In this model, an optimality degree equal to 1 refers to a potential yield with marketable value high-quality fruit. For example, $Opt(T) = 1$ is associated with $T \in [24, 27]^{\circ}\mathrm{C}$ at the vegetative to mature fruiting growth stage during sun hours. For the same growth stage and light condition, a wider reference border, that is, $T \in [18.4, 32.2]^{\circ}\mathrm{C}$, is associated with a lower range of optimality degrees, $Opt(T) \in [0.6, 1]$. In other words, a greenhouse air temperature equal to 32.2°C during sun hours is 60% optimal for tomato production in the vegetative to mature fruiting growth stage. The reference values corresponding to the optimal, marginal, and failure T and RH are summarized in **Table 1**. These values for VPD depend on the range of T and RH and are discussed in Ref. [23]. The optimality-degree model was implemented in the framework as a toolbox and was successfully used in evaluating microclimate parameters. Results of an actual case study on a net-screen-covered greenhouse in tropical lowlands of Malaysia are provided in **Figures 6** and **7** [22].

3.2. Comfort ratio of microclimate

Comfort ratio of a microclimate parameter, denoted by $Cft(\mathcal{M}, t, \alpha_s)_{GS} = \beta$, is defined as the percentage of $\mathcal{M}$ data collected during time frame *t* that falls inside reference borders of $\mathcal{M}$

Temperature			Relative humidity		
Growth stage	**Reference border**	**Value (°C)**	**Growth stage**	**Reference border**	**Value (%)**
Early growth (GS1)	$T1_{\alpha_0 L}$	9	**Early growth (GS1)**	$RH1_{\alpha_0 L}$	60
	$T1_{\alpha_0 H}$	35		$RH1_{\alpha_1 L}$	75
	$T1_{\alpha_1 L}$	24		$RH1_{\alpha_1 H}$	99
	$T1_{\alpha_1 H}$	26.1			
Vegetative to termination (GS2-5)	$T2_{\alpha_0 L}$	10	**Vegetative (GS2)**	$RH2_{\alpha_0 L}$	40
	$T2_{\alpha_0 H}$	40		$RH2_{\alpha_0 H}$	99
	$T2_{\alpha_{0.5}\mathrm{N}}$	17		$RH2_{\alpha_1 L}$	70
	$T2_{\alpha_1 \mathrm{L,N}}$	18		$RH2_{\alpha_1 H}$	80
	$T2_{\alpha_1 H,N}$	20	**Flowering to termination (GS3-5)**		
	$T2_{\alpha_1 \mathrm{L,S}}$	24		$RH3_{\alpha_0 L}$	30
	$T2_{\alpha_1 H,S}$	27		$RH3_{\alpha_0 H}$	99
	$T2_{\alpha_1 L,C}$	22		$RH3_{\alpha_1 L}$	60
	$T2_{\alpha_1 H,C}$	24		$RH3_{\alpha_1 H}$	80

Indices are: L: lower border, H: higher border, N: night, C: cloud, S: sun, α_0: index of failure, $\alpha_{0.5}$: index of Opt=0.5, α_1: index of Opt=1.

Table 1. Reference values of optimal and failure T and RH at different growth stages and light conditions.

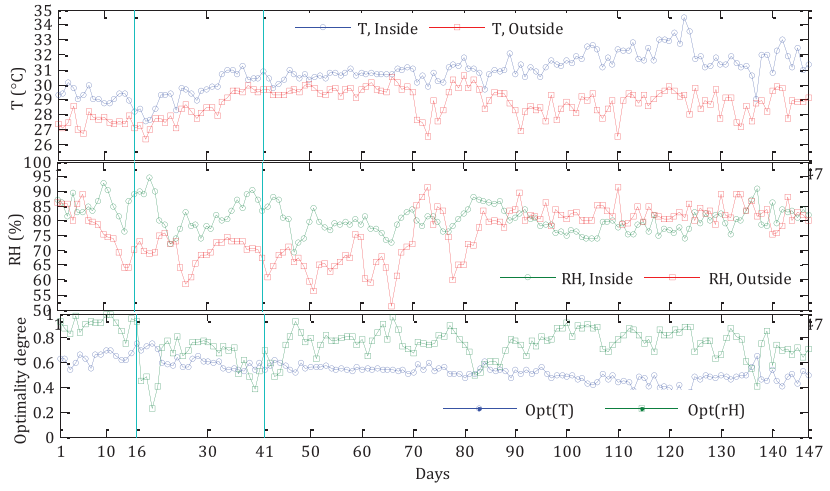

Figure 6. Plots of daily averaged air temperature, RH, and associated optimality degrees from a tropical greenhouse experiment (Source: [22]).

http://dx.doi.org/10.5772/intechopen.69972

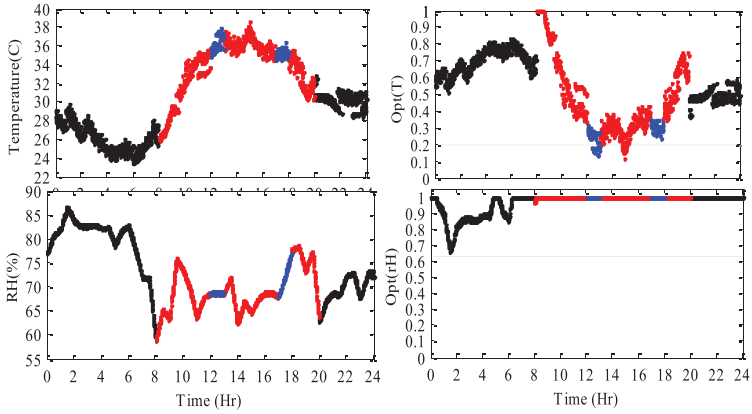

Figure 7. Demonstration of real-time measured air temperature and RH (left) and corresponding optimality degrees (right) for a random cultivation day at the flowering to mature fruiting growth stage (date: March 11, 2015) in a tropical greenhouse. Each color represents a light condition, back: night, red: sun, blue: cloud (Source: [22]).

associated with α_s at a specific growth stage. A 100% ideal microclimate growth condition is therefore defined as $Cft(\mathcal{M}, t, 1) = 1$. The notation α_s refers to user-preferred optimality degree for adjusting the reference borders that is desired for microclimate evaluation or control. The reference borders for a given α_s are calculated from available simulation models (i.e., from the membership function growth response models of [21, 23]). For the purpose of this chapter, mathematical descriptions of Ref. [21] model for defining reference borders of air temperature and relative humidity are adapted and provided in **Table 2**. An example is demonstrated in **Figure 8** for constructing reference borders of air temperature associated with $\alpha_s = 0.8$ at the vegetative to mature fruiting growth stage. The procedure is similar for other microclimate parameters (RH and VPD) at other growth stages and for any selection of $0 \leq \alpha_s \leq 1$. The framework algorithm automatically selects proper membership functions from database according to the light condition and growth stage and computes the reference borders for the given α_s. The light condition in this demonstration belongs to a random day, date: December 15, 2013. The reference borders corresponding to $\alpha_s = 0$, $\alpha_s = 0.8$ and $\alpha_s = 1$ are shown in red, blue, and green colors, respectively. The framework plots data inside each reference border in different colors (black for $\alpha_s = 0$, blue for a preferred α_s, and green for $\alpha_s = 1$). If a measurement lies outside marginal reference borders ($\alpha_s = 0$), it will be plotted in red.

The main purpose of introducing comfort ratio and corresponding graphical demonstration is to address deviation of microclimate responses with respect to different reference borders and to compare it for different cultivation days or greenhouse designs. A practical example is provided in **Figure 9** for air temperature collected from a naturally ventilated greenhouse in two random days, one at the early growth and the other at the mature fruiting stage. The reference borders associated with a preferred optimality degree (i.e., $\alpha_s = 0.7$) are shown in blue color-dashed lines. Moreover, the reference borders corresponding to failure air

Reference function	Preferred optimality
$T(\alpha)_{G1A} = \begin{cases} T1_{\alpha_0 L} \bigwedge T1_{\alpha_0 H} \\ \alpha(T1_{\alpha_1 L} - T1_{\alpha_0 L}) + T1_{\alpha_0 L} \bigwedge \alpha(T1_{\alpha_1 H} - T1_{\alpha_0 H}) + T1_{\alpha_0 H} \\ [T1_{\alpha_1 L}, T1_{\alpha_1 H}] \end{cases}$	$\alpha = 0$ $0 < \alpha < 1$ $\alpha = 1$
$T(\alpha)_{G2S} = \begin{cases} T2_{\alpha_0 L} \bigwedge T2_{\alpha_0 H} \\ \alpha(T2_{\alpha_1 \mathrm{L,S}} - T2_{\alpha_0 L}) + T2_{\alpha_0 L} \bigwedge \alpha(T2_{\alpha_1 \mathrm{H,S}} - T2_{\alpha_0 H}) + T2_{\alpha_0 H} \\ [T2_{\alpha_1 \mathrm{L,S}}, T2_{\alpha_1 \mathrm{H,S}}] \end{cases}$	$\alpha = 0$ $0 < \alpha < 1$ $\alpha = 1$
$T(\alpha)_{G2C} = \begin{cases} T2_{\alpha_0 L} \bigwedge T2_{\alpha_0 H} \\ \alpha(T2_{\alpha_1 L,C} - T2_{\alpha_0 L}) + T2_{\alpha_0 L} \bigwedge \alpha(T2_{\alpha_1 H,C} - T2_{\alpha_0 H}) + T2_{\alpha_0 H} \\ [T2_{\alpha_1 L,C}, T2_{\alpha_1 H,C}] \end{cases}$	$\alpha = 0$ $0 < \alpha < 1$ $\alpha = 1$
$T(\alpha)_{G2N} = \begin{cases} T2_{\alpha_0 L} \bigwedge T2_{\alpha_0 H} \\ 2\alpha(T2_{\alpha_{0.5}\mathrm{N}} - T2_{\alpha_0 L}) + T2_{\alpha_0 L} \\ T2_{\alpha_{0.5}\mathrm{N}} \\ 2\alpha(T2_{\alpha_1 \mathrm{L,N}} - T2_{\alpha_{0.5}\mathrm{N}}) + T2_{\alpha_{0.5}\mathrm{N}} - (T2_{\alpha_1 \mathrm{L,N}} - T2_{\alpha_{0.5}\mathrm{N}}) \\ [T2_{\alpha_1 \mathrm{L,N}}, T2_{\alpha_1 H,N}] \\ \alpha(T2_{\alpha_1 H,N} - T2_{\alpha_0 H}) + T2_{\alpha_0 H} \end{cases}$	$\alpha = 0$ $0 < \alpha < 0.5$ $\alpha = 0.5$ $0.5 < \alpha < 1$ $\alpha = 1$ $0 < \alpha < 1$
$RH(\alpha)_{G1A} = \begin{cases} RH1_{\alpha_0 L} \\ \alpha(RH1_{\alpha_1 L} - RH1_{\alpha_0 L}) + RH1_{\alpha_0 L} \\ RH1_{\alpha_1 H} \end{cases}$	$\alpha = 0$ $0 < \alpha < 1$ $\alpha = 1$
$RH(\alpha)_{G2A} = \begin{cases} RH2_{\alpha_0 L} \bigwedge RH2_{\alpha_0 H} \\ \alpha(RH2_{\alpha_1 L} - RH2_{\alpha_0 L}) + RH2_{\alpha_0 L} \bigwedge \alpha(RH2_{\alpha_1 H} - RH2_{\alpha_0 H}) + RH2_{\alpha_0 H} \\ [RH2_{\alpha_1 L}, RH2_{\alpha_1 H}] \end{cases}$	$\alpha = 0$ $0 < \alpha < 1$ $\alpha = 1$
$RH(\alpha)_{G3A} = \begin{cases} RH3_{\alpha_0 L} \bigwedge RH3_{\alpha_0 H} \\ \alpha(RH3_{\alpha_1 L} - RH3_{\alpha_0 L}) + RH3_{\alpha_0 L} \bigwedge \alpha(RH3_{\alpha_1 H} - RH3_{G0,\max}) + RH3_{\alpha_0 H} \\ [RH3_{\alpha_1 L}, RH3_{\alpha_1 H}] \end{cases}$	$\alpha = 0$ $0 < \alpha < 1$ $\alpha = 1$

Table 2. Membership function model for adjusting reference borders of air temperature and RH.

temperature ($\alpha_s = 0$) and optimum air temperature ($\alpha_s = 1$) are, respectively, shown in red- and green-dashed lines. In this example, the percentage of data that falls inside these three reference borders ($\alpha_s = 0$, 0.7 and 1) are 100, 92 and 41% for the early growth stage, and 100, 73, and 3% for the mature fruiting stage. These values are expressed on the plots of **Figure 9** as $Cft(T, 24, 0)_{GS1} = 1$, $Cft(T, 24, 0.7)_{GS1} = 0.92$, $Cft(T, 24, 1)_{GS1} = 0.41$, $Cft(T, 24, 0)_{GS5} = 1$, $Cft(T, 24, 0.7)_{GS5} = 0.73$, and $Cft(T, 24, 1)_{GS5} = 0.03$. In other words, $Cft(T, 24, 0.7)_{GS1} = 0.92$ and $Cft(T, 24, 0.7)_{GS5} = 0.73$ imply that for nearly 22 h (92% of the entire 24 h) of the random day at the early growth, and for 17.5 h (73% of the entire 24 h) of the random day at the mature fruiting stage, the climate controller (for this example, natural ventilation) provided the greenhouse with air temperature that was at least 70% optimal for tomato cultivation. Moreover, $Cft(T, 24, 1)_{GS1} = 0.41$ implies that at the early growth stage, the greenhouse was controlled

http://dx.doi.org/10.5772/intechopen.69972

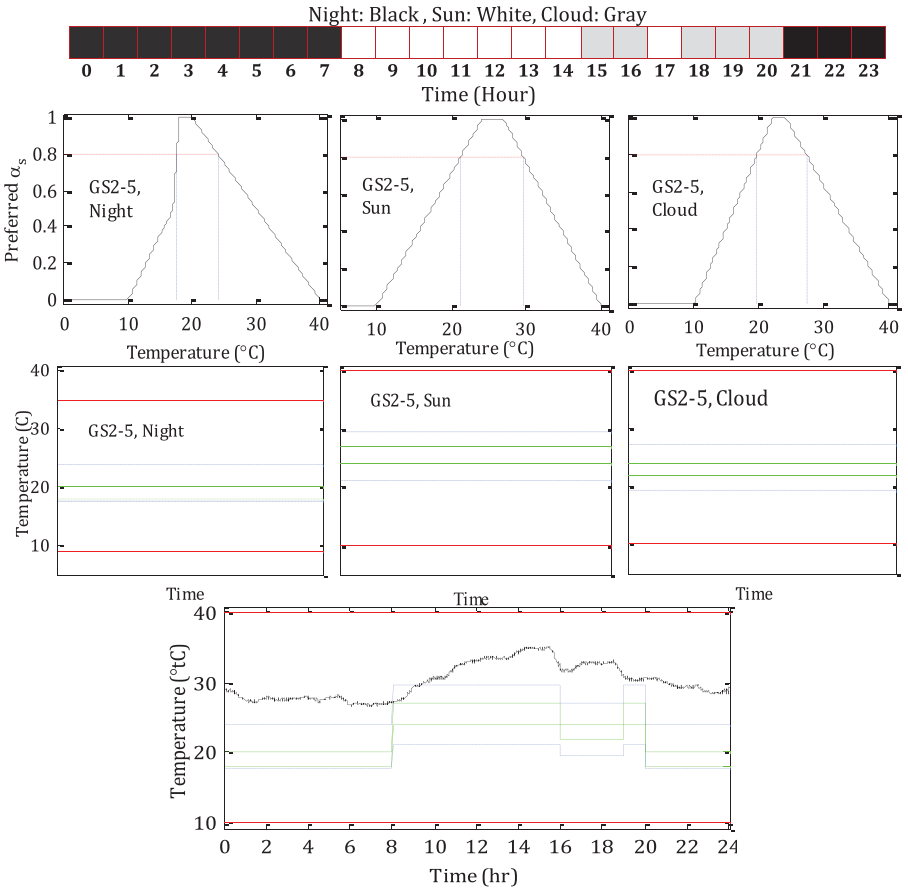

Figure 8. Demonstration of adjusting reference borders with light condition and a preferred optimality degree of $\alpha = 0.8$ for air temperature control and evaluation in a random day at the flowering to mature fruiting growth stage.

with 100% optimal air temperature for a total of 9.6 h (41% of the total 24 h, shown by green color between hours of 00:00–11:00 on the left plot of **Figure 9**). For the random day at the mature fruiting stage, it can be seen that only 3% of the air temperature response is inside $\alpha_s = 1$ reference borders (around hour 8:00 to 8:30 am).

The discussion for comfort ratio is extended to compare VPD response in three different greenhouses for a random data collection day during the flowering growth stage (GS3). The greenhouses had different covering materials and climate control system (labeled by A, B, and C in **Figure 10**, respectively, covered with net-screen mesh, polyethylene film, and polycarbonate panels). The preferred reference border for this evaluation is $\alpha_s = 0.6$ (blue-color borders). It can be observed that VPD response never crossed $\alpha = 0$ or the failure reference borders in greenhouses A and C. This can be expressed by saying that $Cft(VPD, 24, 0)_{GS3}$ was never less

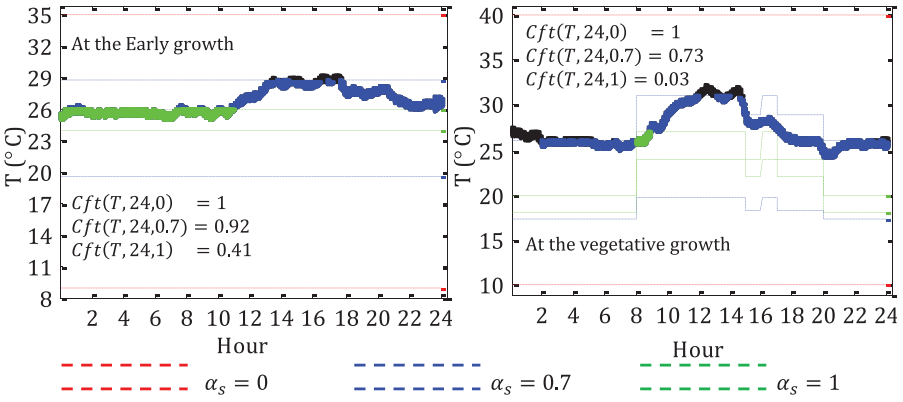

Figure 9. Demonstration of air temperature response and corresponding comfort ratios for two random days of experiment at the early growth (left) and mature fruiting stage (right) in a tropical greenhouse.

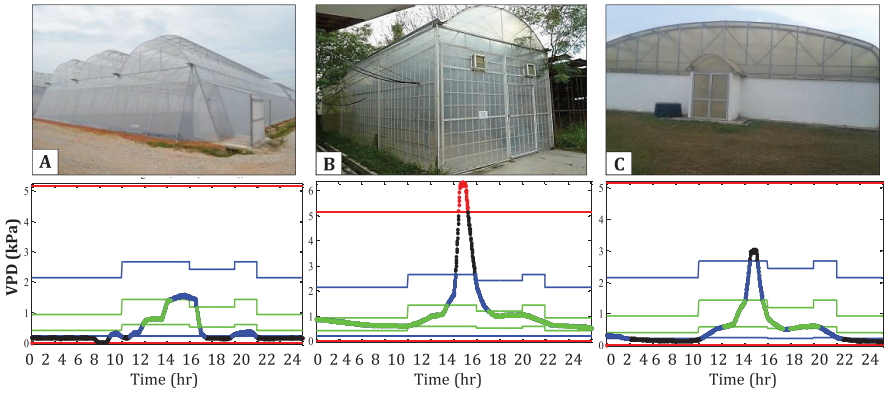

Figure 10. A comparison between comfort ratio of VPD at reference borders of $\alpha = 0$, $\alpha = 0.6$, and $\alpha = 1$ in three different greenhouses. Date of data collection March 18, 2013.

than 1 in greenhouses A and C. It should be mentioned that these two greenhouses were, respectively, operating on natural ventilation and evaporative cooling system during the experiment. According to the plots of the three greenhouses in **Figure 10**, no significant difference can be observed in their VPD responses between 0.1 and 1.2 kPa (corresponding to air temperature between 20 and 30°C, and RH between 80 and 100%); however, as air temperature starts rising above 30°C, differences in the environments start growing nonlinearly. The hourly averaged values of microclimate parameters for this experiment reveal that the major differences between these greenhouses occur between hours of 11:30 am to 4:00 pm. The mean VPD value for greenhouses B and C was equal to 2.9 and 1.19 kPa, respectively, which are less desirable for plant growth compared with the 0.97-kPa value observed from greenhouse A.

This observation indicates that as long as the outside temperature is less than 30°C, no major differences between the three greenhouses resulted. This example indicates that for this particular day of experiment, the net-screen-covered greenhouse operating on natural ventilation had a comfort ratio equal to 1 at $\alpha_s = 0.6$, which is slightly higher than $Cft(T, 24, 0.6)_{GS5} = 0.95$ of the polycarbonate panel greenhouse with evaporative cooling system. It should be noted that greenhouse C was constructed with more expensive materials, including polycarbonate panels to reduce direct sun radiation, and was operating on evaporative cooling system with large fans that consume substantial amount of electricity. This example clearly shows the potential of natural ventilation in providing more desirable response for tomato cultivation under tropical climate conditions.

3.3. Simulation of expected yield

A peer-reviewed published state-variable tomato growth model, developed by Ref. [24] in Microsoft Excel spreadsheets, was studied and implemented in MATLAB Simulink (shown by Simulink blocks in **Figures 11–13**). The objective was to provide a standalone application in a way that end users unfamiliar with programming languages and/or crop modeling would have an easier access to yield prediction in different greenhouse environments. Data from spreadsheet version of the model were used for testing the Simulink blocks and validation of the results [25]. The five state variables included in the tomato growth model of Ref. [24] were node number (N), leaf area index (LAI), total plant weight (W) or biomass, total fruit weight (W_F), and mature fruit weight (W_M). Vegetative node development is calculated on an hourly time step using greenhouse temperature (T). The state-variable equation for the rate of node development (dN/dt) is expressed by $dN/dt = N_m.f_N(T)$, where N_m is the maximum rate of node appearance per day and $f_N(T)$, is a function to reduce node development under nonoptimal temperatures on an hourly basis. Based on studies of tomato phenology, N_m was established to be 0.02083 $nodes.d^{-1}$ in the model, and the function, $f_N(T)$, is $f_N(T) = \min(1, \min(0.25 + 0.025T, 2.5 - 0.05T))$, where T is the hourly greenhouse temperature in °C. Gross hourly photosynthesis (P_h) was calculated as a function of hourly temperature, incoming solar radiation, and LAI using Eq. (1) developed by Ref. [26]. The Simulink blocks for hourly node development and hourly photosynthesis are shown in **Figure 11**. Here, D is a coefficient to convert P_h from $\mu mol(CO_2)m^{-2}.\,s^{-1}$ to $g(CH_2O)m^{-2}.\,d^{-1}$, K is the light extinction coefficient, m is the leaf light transmission coefficient, $LF_{\max}$ is the maximum leaf photosynthetic rate, $Q_e(T)$ is the leaf quantum efficiency and a function of temperature, $PPFD$ is the photosynthetic photon flux density or the level of incoming solar radiation, and $PGRED(T)$ is a function to modify P_h under suboptimal temperatures. Based on previous work with tomato growth models [24], D, K, m, and $LF_{\max}$ were set to 0.108, 0.58, 0.1, and 26, respectively. The function for $Q_e(T)$ can be expressed by $Q_e(T) = 0.084\ .\ \left(1 - 0.143\exp\left(0.0295.(T - 23)\right)\right)$.

The function for $PGRED(T)$ was disregarded for this model because environmental conditions inside a greenhouse will not fluctuate significantly enough such that this function would have an effect on tomato growth simulations. Temperature and incoming solar radiation information necessary for computation of P_h were obtained from hourly measured data in

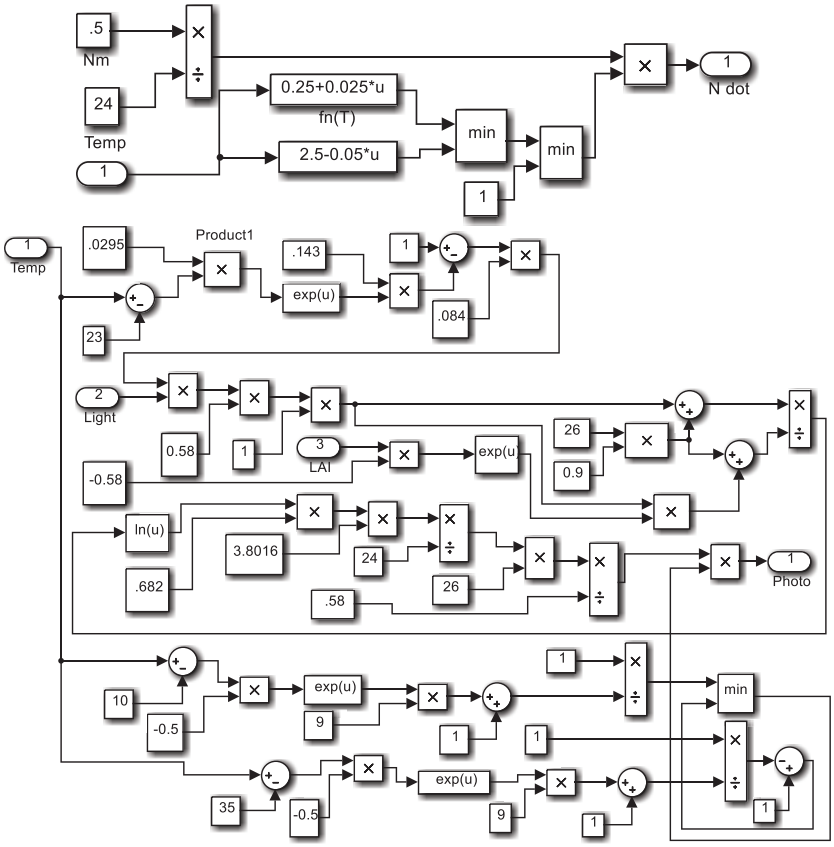

Figure 11. Simulink blocks for hourly node development and hourly photosynthesis.

the greenhouses under study, and LAI was obtained using a feedback loop in the model. Gross daily photosynthesis (P_g) was found by integrating over the 24-hourly photosynthesis calculations during each day. Hourly maintenance respiration (R_h) was computed as $R_h = r_m.Q_{10}^{(T-20)/10}$, where r_m and Q_{10} are maintenance respiration coefficients for tomato with values of 0.019 and 1.4, respectively. Daily maintenance respiration (R_m) was computed by integrating over the 24-hourly respiration calculations during the day. Vegetative node development was the only state variable computed on an hourly time step. The remaining state variables were calculated on a daily time step. The state-variable equation for computing LAI was derived from the work of [27, 28]. This state-variable equation is expressed by Eq. (2), where ρ is the plant density, $\lambda(T_d)$ is a function to reduce the rate of leaf area expansion for nonoptimal temperatures, and δ, β, and N_b are coefficients in the expolinear growth equation developed by Ref. [27]. For this work, the values for ρ, δ, β, and N_b were 3.12 plants m^{-2}, 0.038 m^{-2} $node^{-1}$, 0.169 $node^{-1}$, and

http://dx.doi.org/10.5772/intechopen.69972

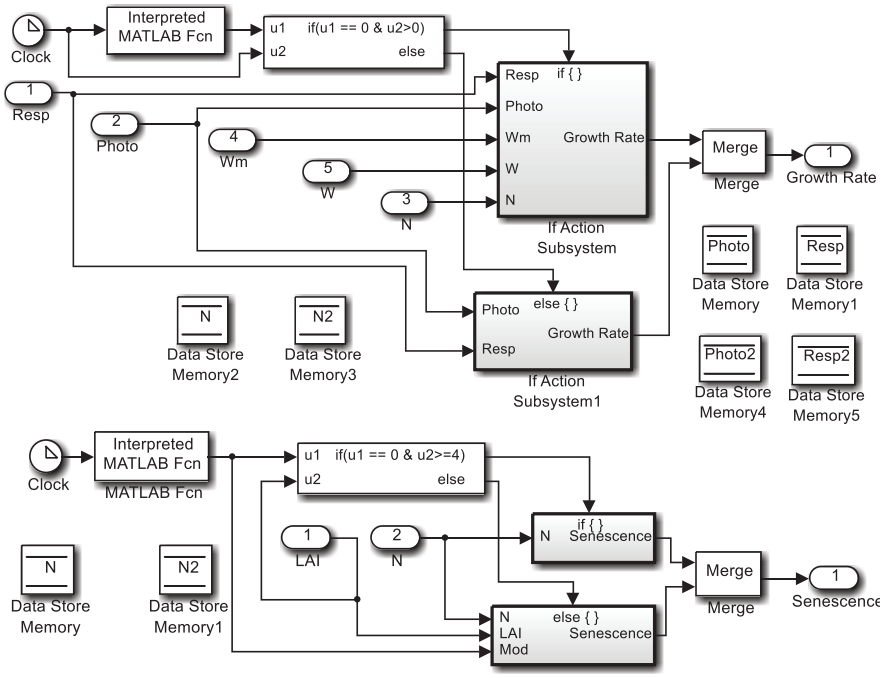

Figure 12. Simulink blocks for daily biomass accumulation and senescence.

16 nodes, respectively. The function, $\lambda(T_d)$, was not necessary for this model because temperatures within a greenhouse will not fluctuate enough for this function to significantly affect leaf area expansion simulations. The value for N is the node count at the end of the previous day, and dN/dt is the change in node count during the current day. The model assumes that when LAI reaches LAI_{max}, any additional leaf growth will be either pruned or senesced to maintain LAI at a constant value for the remainder of the growing period. For this work, the value of LAI_{max} was set to 4 as recommended by Ref. [24]. The state-variable equation for computing the accumulation of aboveground biomass (W) is based on the equation for daily plant growth (GR_{net}), that is, $GR_{\text{net}} = E.\left[P_g - R_m(W - W_M)\right].\left[1 - f_R(N)\right]$. Here, $(W - W_M)$ is the difference between the total aboveground biomass and the total mature fruit, and this difference represents the growing and respiring plant mass. This difference is multiplied by the daily respiration rate (R_m) to get the amount of carbon necessary for plant maintenance. Subtracting this value from the total carbon assimilated during the day (P_g) gives the total carbon available for plant growth. The coefficient, E, represents the efficiency at converting photosynthate to crop biomass, and this value was set to 0.75 in this work. The function, $f_R(N)$, determines the proportion of carbon that is partitioned to roots as a function of the number of nodes, and it can be expressed as $f_R(N) = \max(0.02, 0.18 - 0.0032.N)$. The function allows a relatively large portion of carbon to

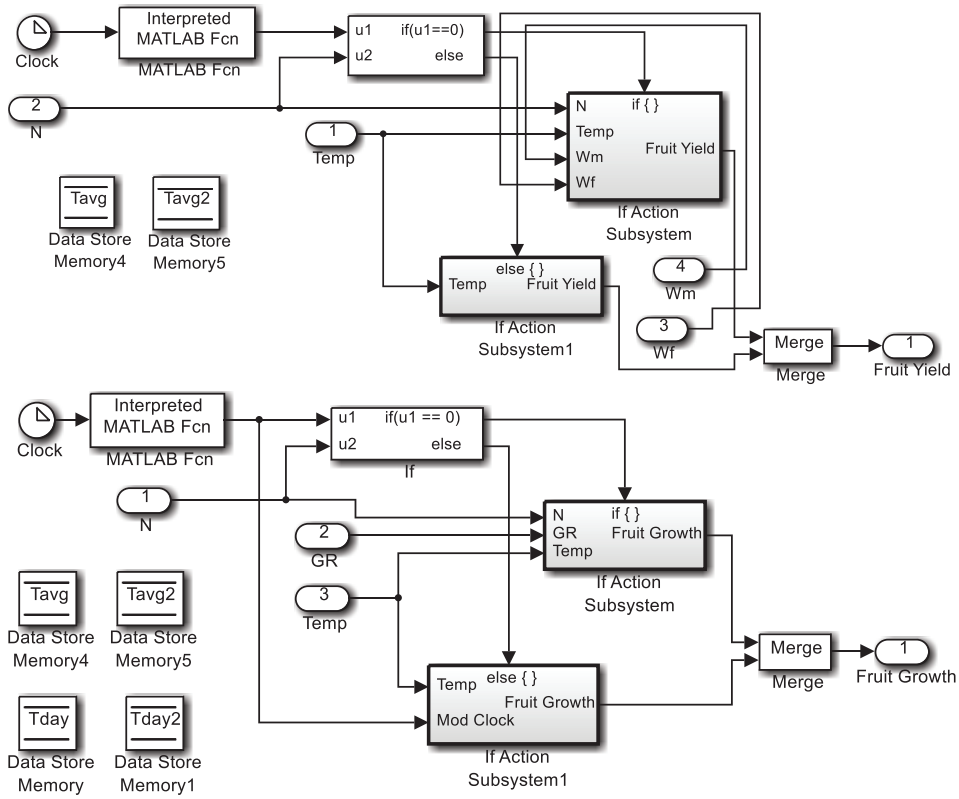

Figure 13. Simulink blocks for daily mature fruit weight and daily fruit growth.

be allocated to roots when the plant is young, and this portion tapers off to 0.02 as the plant matures. The state-variable equation for computing the accumulation of aboveground biomass (W) is $dW/dt = GR_{\text{net}} - p_1.\rho.dN/dt$, where p_1 is the dry matter weight of leaves removed per day due either to senescence or to pruning after LAI_{max} is achieved. For this work, the value of p_1 was 0 $g.node^{-1}$ before LAI_{max} was reached and 2 $g.node^{-1}$ after LAI_{max} was reached. The state-variable equation to calculate the total fruit weight (W_F) is expressed by Eq. (3). Simulink blocks for daily biomass accumulation and senescence are shown in **Figure 12**.

Here, α_F is the maximum partitioning of new growth to fruit, $f_F(T_d)$ is a function to modify partitioning to fruit according to the average daily temperature (T_d), ϑ is the transition coefficient between vegetative and full fruit growth, N_{FF} is the nodes per plant when the first fruit appears, and $g(T_{\text{daytime}})$ is a function to reduce fruit growth due to high daytime temperature. For this work, $\alpha_{F,}$ ϑ, and N_{FF} were 0.95 d^{-1}, 0.2 $node^{-1}$, and 10 nodes, respectively. The function $f_F(T_d)$ is expressed as $f_F(T_d) = \max(0, \min(1, 0.0625.(T_d - T_{\min})))$, where $T_{\min}$ is the minimum

temperature below which no fruit growth occurs. The function $g(T_{\text{daytime}})$ is expressed by Eq. (4) where T_{daytime} is the average temperature during daylight hours and T_{crit} is the temperature above which fruit abortion begins. For tomato, T_{min} and T_{crit} are 8.5 and 24.4°C, respectively. The state-variable equation to calculate the total weight of mature fruit or the total tomato yield is expressed by Eq. (5) where $D_F(T_d)$ is a function for the rate of fruit development according to the average daily temperature, and κ_F is the development time from first fruit to first ripe fruit. For this work, κ_F was five nodes, and the function, $D_F(T_d)$, is expressed as $D_F(T_d) = 0.04\ .\max(0, \min(1,\ 0.0714.(T_d - 9)))$. Mature fruit is assumed to be harvested from the plants immediately upon ripening, as shown by the subtraction of W_M during each time step from net crop growth explained by GR_{net} equation. Simulink blocks for daily mature fruit weight and daily fruit growth are shown in **Figure 13**. This description completely explicates the reduced state-variable tomato model implemented in Simulink for this project, and the state-variable equations for LAI, total biomass accumulation (dW/dt), total fruit weight (dW_F/dt), and mature fruit weight ((dW_M/dt)) are highlighted. The implemented model was validated [25] using the Lake City experiment datasets of Ref. [24] to show that the Simulink version of the model is an exact replication of the original spreadsheet version. It was then used in yield prediction from the three greenhouses shown in **Figure 10**. Results of the prediction are summarized in **Figure 14**, showing that the net-screen greenhouse operating on natural ventilation (greenhouse labeled A) had the highest yield compared with the polycarbonate panel and polyethylene film greenhouses. This result is completely consistent with results of the optimality degrees and comfort ratios obtained in the previous sections.

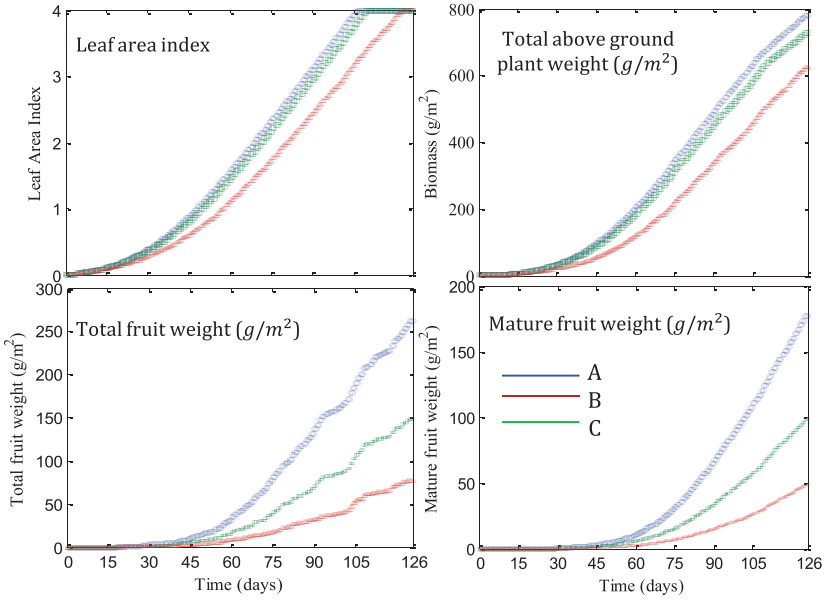

Figure 14. Simulated results with TOMGRO model for three experimental greenhouses.

4. Set-point manipulation for optimum climate control

4.1. Critical reference borders

The comfort ratio curve, denoted by Cft- curve, refers to the plot of $Cft(\mathcal{M}, t, \alpha_s)$ values calculated for all $\alpha_s = 0 : d_\alpha : 1$. It shows how much close a microclimate parameter can be controlled to different preferred reference borders. The horizontal blue-dashed line at $Cft(\mathcal{M}, t, \alpha_s) = 1$ represents 100% satisfied control objective; that is, parameter $\mathcal{M}$ is always inside reference borders of α_s. The Cft- curve can be used as a tool to demonstrate the behavior of $Cft(\mathcal{M}, t, \alpha_s)$ in different greenhouses or at different cultivation days for decision making in set-point manipulation for the climate controller. For example, it can be used in finding the largest α_s for which $Cft(M, t, \alpha_s) = 1$ (in other words, finding $\alpha_{\max}$ corresponding to the narrowest achievable reference border by the climate controller). An example is provided in **Figure 15** by plotting air temperature response for 2 consecutive days of an experiment inside a tropical greenhouse. It can be observed that the narrowest reference borders of air temperature that was completely satisfied by the climate controller in these two days are, respectively, equal to $\alpha_s = 0.55$ and $\alpha_s = 0.67$. After these points, comfort ratio starts decreasing until it arrives at its lowest value of 0.42 for both days at $\alpha_s = 1$.

Another application of the Cft- curve includes finding critical reference borders, denoted by α_{Crit} at which $\Delta = Cft(\mathcal{M}, t, \alpha_s) - Cft(\mathcal{M}, t, \alpha_s + \epsilon)$ is maximum (reference borders that cause significant loss in comfort ratio). To further explain, comfort ratios of air temperature for two distinct cases are plotted in **Figure 16**. In the first case, increasing α_s from 0.3 to 0.65 has not caused significant loss in the resulting comfort ratio. The values of $Cft(T, t, 0.3)$ and $Cft(T, t, 0.75)$ for this case are nearly the same and equal to 0.8 and 0.77. In other words, by increasing α_s from 0.3 to 0.75 to provide air temperature response that is more favored by tomato plants, performance of the controller in achieving the extra accuracy was not decreased. In a greenhouse with natural ventilation, this means that the extra 0.35 increase in α_s comes at no cost (no significant loss of response). In the case of an energy-consuming climate controller (i.e., pad-and-fan-evaporative system or swamp cooler), it means that the

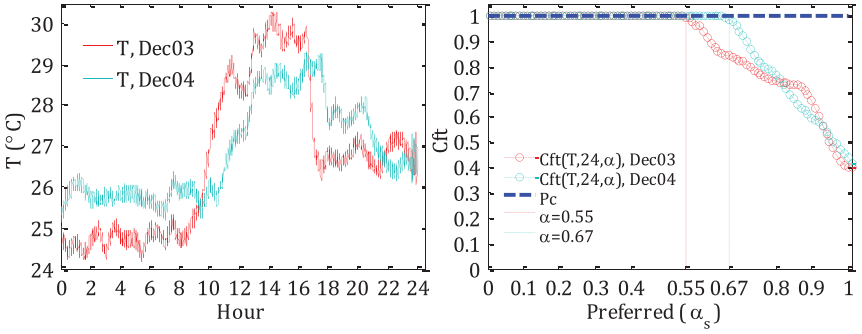

Figure 15. Comparison between air temperature responses from a tropical greenhouse in 2 days of experiment showing raw data (left), and comfort ratios (right). The controller did not satisfy 100% optimal references.

http://dx.doi.org/10.5772/intechopen.69972

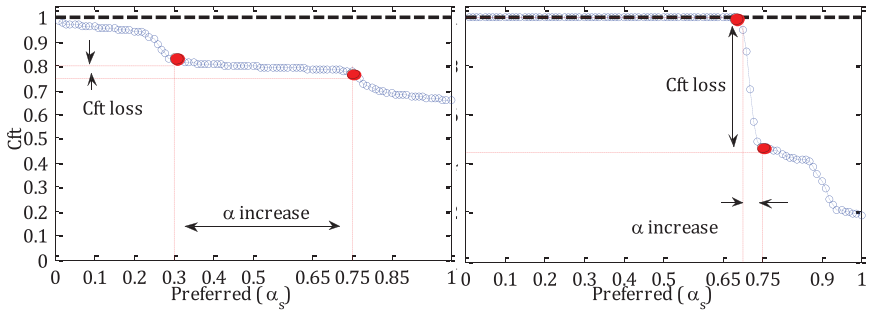

Figure 16. Comparison between comfort ratios versus α_s in 2 days of experiment in a greenhouse with evaporative cooling system for demonstration of α_{Crit}. Left: significant increase in α_s from 0.3 to 0.75 resulting in significant loss in Cft, right: slight increase in α_s from 0.7 to 0.75 causing significant loss in Cft.

cooler can be set to maintain air temperature inside a narrower reference border (by selecting $\alpha_s = 0.75$ rather than 0.3) without imposing additional energy cost. On the right plot of **Figure 16**, this situation is, however, different. Significant loss in $Cft(T, t, \alpha_s)$ can be observed for a slight increase from $\alpha_s = 0.7$ to $\alpha_s + \epsilon = 0.75$. Here, increasing α_s for as little as 0.05 has led to a sudden drop in the comfort ratio by 50% (from 1 to 0.5). The α_s at which the largest loss appear is referred to α_{Crit} and can be calculated by differentiating Cft -curve with respect to α as $\alpha_{\text{crit}} = d/d_\alpha(Cft(\mathcal{M}, t, \alpha))$.

4.2. Performance of climate controller

Plots of measured optimality degrees of a response parameter, denoted by $Opt(\mathcal{M}) = \alpha_y$, corresponding to the preferred α_s reference borders can provide a useful graphical tool to monitor performance of the climate control system. For the sake of demonstration, Cft- curves and performance curves of the climate controller for T, RH, and VPD are shown in **Figure 17**. For a perfectly control task with a preferred α_s, the control system must achieve microclimate parameter $\mathcal{M}$ that has optimality degree of at least α_s. For example, if reference borders of air temperature control are set at $\alpha_s = 0.8$, it is expected that the optimality degree of air temperature response inside the greenhouse is at least $\alpha_y = 0.8$ at any measured time. As mentioned earlier, in a 100% perfectly controlled greenhouses, the measured optimality degrees are at least equal to the preferred optimality degrees of the reference border ($\alpha_y = \alpha_s$). This is shown by the perfect control line (line of $\alpha_y = \alpha_x$) on the response plot of **Figure 17**. It should be noted that α_y can also be calculated by integrating $Cft(\mathcal{M}, t, \alpha)$ curve over $\alpha = 0$ to $\alpha = \alpha_s$ (Eq. (6)), indicating that α_y is equal to α_s only when $Cft(\mathcal{M}, t, \alpha_s)$=1. In other words, performance of a climate control system in achieving preferred reference borders of $\mathcal{M}$ is considered 100% perfect only when 100% of $\mathcal{M}$-response falls inside the α_s preferred optimal reference borders.

In controlled greenhouses, both *Cft curve* and performance curve provide a graphical assessment tool for comparing different control strategies and scenarios (i.e., microclimate responses due to different greenhouse designs, cooling systems, and covering materials at different

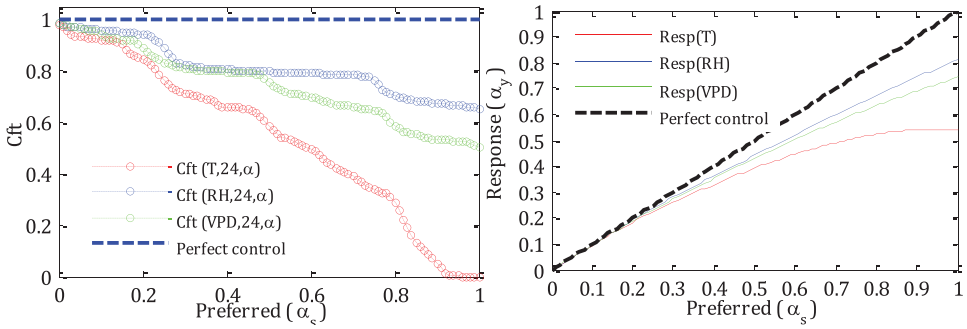

Figure 17. Comfort ratio of microclimate parameters (left) and response of the climate controller (right) at $0 \leq \alpha_s \leq 1$.

growth stages). The performance curve in fact reveals how much a greenhouse microclimate parameter deviates from a perfectly controlled response. Deviation of the greenhouse from this ideal line at any α_s can be used as an index factor of the perfect climate control task. The lesser deviation means the more perfect control task. Adaptability factor of the controller for microclimate parameter $\mathcal{M}$ at a preferred α_s, denoted by $ADP(\mathcal{M}, \alpha_s)$, is then defined as the ability of the controller to adapt itself with different preferred references and is calculated using Eq. (7).

4.3. Optimum reference borders

The optimum preferred reference border for parameter $\mathcal{M}$, denoted by α_{Opt}, is defined as the largest possible α_s value for which the largest $Cft(\mathcal{M}, t, \alpha)$ can be achieved. In other words, it is the value of an unknown α_i for which $Cft(\mathcal{M}, t, \alpha_i) = \beta_i$ has the minimum distance to $Cft(\mathcal{M}, t, 1) = 1$. In that sense, the cost function for this optimization problem is defined as $D_i = \sqrt{(\alpha_i - 1)^2 + (\beta_i - 1)^2}$, which is the Euclidean distant between the unknown point (α_i and β_i) on the *Cft curve* and the point of ideal microclimate ($\alpha = 1$ and $\beta = 1$). The objective is

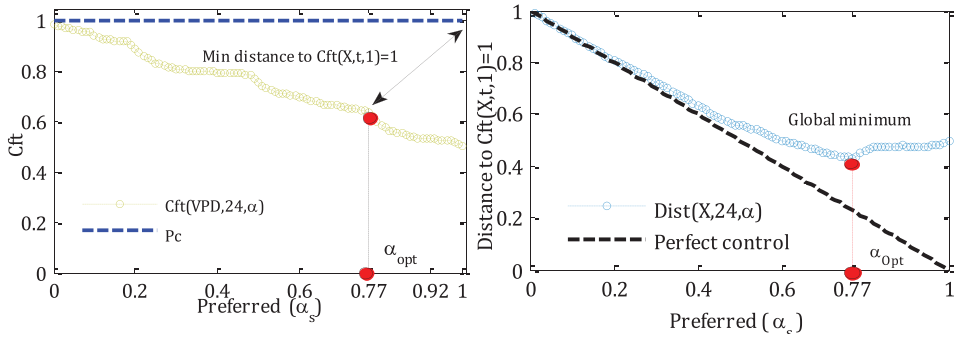

Figure 18. Demonstration of the algorithm for finding optimum preferred reference border for adjusting the climate controller. Data belongs to VPD response from a random data collection day in a tropical greenhouse experiment.

therefore to minimize this cost function by finding $0 \leq \alpha_i \leq 1$ value that leads to the shortest Euclidean distant (minimum $Dist_i$) to the $Cft(\mathcal{M}, t, 1) = 1$. An example is demonstrated in **Figure 18** for VPD response in a random day of experiment with $\alpha_{\text{Opt}} = 0.77$. The plot on the right side of **Figure 18** shows the values of D_i versus $0 \leq \alpha_i \leq 1$, and the position of α_{Opt} is shown as the global minimum point.

5. Conclusion

An adaptive management framework was designed, developed, and introduced in this research to respond to the needs for an iterative processing tool that acknowledge complexity and uncertainty in microclimate control and management. A systematic approach was presented for automatic data collection and processing with the objective to produce knowledge-based information in achieving optimum microclimate for producing high-quality and high-yield tomato. Applications of computer models were demonstrated through case-study examples for measuring and adjusting optimality degrees, comfort ratios, and prediction of the expected yield. Several applications of the framework toolboxes were demonstrated through case-study examples for evaluating and comparing microclimate parameters as well as yield prediction in different greenhouse environments. Specific applications of the optimization toolbox of the framework were discussed for evaluating and adjusting greenhouse climate controller through manipulated set points. It was shown that using adaptive greenhouse model for tropical climate condition, efficient use of natural ventilation, or shading will cause up to 70% savings on other energy-consuming cooling systems without sacrificing fruit quality or yield. The presented approach can be used in cost-benefit analysis for providing best management decisions such as site selection, optimum growing season, scheduling efficiencies, energy management with different climate control systems, and risk assessments associated with each task. Results of microclimate evaluation and yield prediction that are generated by this framework can be used in other crop models that estimate plant responses to the environment, or contribute to task-planning algorithms for hierarchical decomposition of climate management, and in economic models of tomato for energy conservation and energy efficient greenhouse crop productions. The framework can also be used as a research tool in future studies such as evaluating effects of different greenhouse designs and shapes on comfort ratios of microclimate parameters, or finding optimum combination of ventilation and evaporative cooling systems for best fruit quality and yield.

6. Technical data

The custom-designed data acquisition and control system [17] for monitoring and manipulating of the microclimate parameters was built using Arduino Uno prototype board utilizing ATmega328P (Atmel®, San Jose, CA) microcontroller on the open source Arduino Uno prototyping platform programmable in Arduino sketch environment software with C (C Compiler, Brookfield, WI), a liquid crystal display, power supply, and serial port RS-232

communication cable (bidirectional with a maximum baud speed up to 115,200 bites per seconds) for transferring and storing collected data in PC. All vital components (i.e., clock generator, 2 KB of RAM, 32 KB of flash memory for storing programs and 1 KB of EEPROM for storing parameters, a 16-MHz crystal oscillator, digital input/output pins, USB connection, power regulator, power jack, and a reset button) for operating the microcontroller, as well as direct programming and access to input/output pins, were available on the prototype board. Four arrays of HSM-20G-combined sensors modules (Shenzhen Mingjiada Electronics LTD, Futian Shenzhen, China), external micro-secure digital (SD) cardboard for storing larger amount of sensor data, output connection, sensor input, and relay circuit board for on/off control purposes were used. The data acquisition interface was tested for accuracy and reliability with available commercial models, and with a control sample data collected from airport weather station at Sultan Abdul Aziz Shah-Subang in Malaysia.

$$P_h = \frac{D\ .\ LF_{max}\ .\ PGRED(T)}{K}.ln\left[\frac{(1-m).LF_{max}+Q_e(T)\ .\ K.\ PPFD}{(1-m)\ .\ LF_{\max}+Q_e(T).\ K.\ PPFD\ .\ exp(-k\ .\ LAI)}\right] \tag{1}$$

$$\begin{cases}\dfrac{d(LAI)}{dt}=\rho.\delta.\lambda(T_d).\dfrac{exp\left[\beta.(N-N_b)\right]}{1+\exp\left[\beta.(N-N_b)\right]}.\dfrac{dN}{dt} & :\ LAI\le LAI_{\max}\\ \dfrac{d(LAI)}{dt}=0 & :\ LAI\ge LAI_{\max}\end{cases} \tag{2}$$

$$\frac{dW_F}{dt}=GR_{net}.\alpha_F.f_F(T_d).\left[1-\exp\left(-\vartheta(N-N_{FF})\right)\right].g\left(T_{daytime}\right)\ if\ N>N_{FF} \tag{3}$$

$$g\left(T_{daytime}\right)=\max\left(0.09,\min\left(1,1-0.154\left(T_{daytime}-T_{crit}\right)\right)\right) \tag{4}$$

$$\frac{dW_M}{dt}=D_F(T_d).(W_F-W_M),\ if\ N>N_{FF}+\kappa_F \tag{5}$$

$$\alpha_y=\int_{\alpha=0}^{\alpha=\alpha_s}Cft(\mathcal{M},t,\alpha).d\alpha=\sum_{i=1}^{N}Cft(\mathcal{M},t,\alpha_i)\times\alpha_i \tag{6}$$

$$ADP(\mathcal{M},\alpha_s)\ =1-2\left(\int_{\alpha=0}^{\alpha=\alpha_s}\alpha.d\alpha-\int_{\alpha=0}^{\alpha=\alpha_s}Opt(\mathcal{M}).d\alpha\right) \tag{7}$$

Acknowledgements

The financial support provided by the University of Putra Malaysia, Grant Number GP-IPB/2013/9415600, and the scientific comments and suggestions from Professor Warren Dixon, Professor Jim Jones, and Professor Ray Bucklin at the University of Florida, and Professor Jan Bontsema at the Wageningen University and Research Center are duly acknowledged.

http://dx.doi.org/10.5772/intechopen.69972

Author details

Redmond R. Shamshiri[1,2]*, Muhammad Razif Mahadi[2], Kelly R. Thorp[3], Wan Ishak Wan Ismail[2], Desa Ahmad[2] and Hasfalina Che Man[2]

*Address all correspondence to: Redmond@AdaptiveAgroTech.com

1 Department of Agricultural and Biological Engineering, University of Florida, Gainesville, FL, USA

2 Department of Biological and Agricultural Engineering, Faculty of Engineering, Universiti Putra Malaysia, Serdang, Selangor, Malaysia

3 United States Department of Agriculture, Agricultural Research Service, Maricopa, AZ, USA

References

[1] Ting, K.C. Automation for Phytomation Systems on Instrumentation and Information Technology for Bioproduction Systems. Invited lecture. Tokyo Institute of Agriculture and Technology, Tokyo, Japan. 1999.

[2] Ting KC, Fleisher DH, Rodriguez LF. Concurrent science and engineering for phytomation systems. Journal of Agricultural Meteorology. 2003;**59**(2):93–101

[3] Ting, K.C. A Systems Concept for Controlled Environment Plant Production. Resource Magazine. Volume March/April. Page 26. Published by the American Society of Agricultural and Biological Engineering (ASABE). 2013. Available online at: http://bt.e-ditionsbyfry.com/publication/index.php?i=148288&m=&l=&p=1&pre=&ver=html5#{"page":26,"issue_id":148288}Last accessed on July 10, 2017

[4] Fleisher DH, Baruh H. An optimal control strategy for crop growth in advanced life support systems. Life Support & Biosphere Science. 2001;**8**(1):43–54

[5] Fleisher DH, Ting KC. Object-oriented analysis and modeling of closed plant production systems. In: Transplant Production in the 21st Century. The Netherlands: Kluwer Academic Publishers; 2001. pp. 53–58

[6] Fleisher DH, Ting KC, Giacomelli GA. Decision support software for phytoremediation systems using rhizofiltration processes. Transactions of the Chinese Society of Agricultural Engineering. 2002;**18**(5):210–215

[7] Holling CS. Adaptive Environmental Assessment and Management. Chichester: Wiley; 1978

[8] Linkov I, Satterstrom FK, Kiker G, Batchelor C, Bridges T, Ferguson E. From comparative risk assessment to multi-criteria decision analysis and adaptive management: Recent developments and applications. Environment International. 2006;**32**(8):1072–1093

[9] Henriksen H, Barlebo H. Reflections on the use of Bayesian belief networks for adaptive management. Environmental Management. 2008;**88**(4):1025–1036

[10] Williams BK. Adaptive management of natural resources—Framework and issues. Journal of Environmental Management. 2011;**92**:1346–1353

[11] Whicker JJ, Janecky DR, Doerr TB. Adaptive management: A paradigm for remediation of public facilities following a terrorist attack. Risk Analysis. 2008;**28**(5):1445–1456

[12] Stankey GH, Bormann BT, Ryan C, Shindler B, Sturtevant V, Clark RN, Philpot C. Adaptive management and the Northwest forest plan: Rhetoric and reality. Journal of Forestry. 2003;**101**(1):40–46

[13] Stankey GH, Clark RN, Bormann BT. Adaptive management of natural resources: Theory, concepts, and management institutions. In: General Technical Report PNW-GTR-654. Portland, OR, USA: U.S. Department of Agriculture, Forest Service, Pacific Northwest Research Station; 2005

[14] Nian-Feng W, Chen J, Jie-Xian J, Li B. A conceptual framework for ecosystem management based on tradeoff analysis. Ecological Indicators 2017;**75**(April):352–361. DOI: http://dx.doi.org/10.1016/j.ecolind.2016.12.032

[15] Aiello, G., Giovino, I., Vallone, M., Catania, P., & Argento, A. A decision support system based on multisensor data fusion for sustainable greenhouse management. Journal of Cleaner Production. 2017. https://doi.org/10.1016/j.jclepro.2017.02.197

[16] McLain RJ, Lee RG. Adaptive management: Promises and pitfalls. Environmental Management. 1996;**20**(4):437–448

[17] Shamshiri R, Wan Ismail WI. Data acquisition for monitoring vapor pressure deficit in a tropical lowland shelter-house plant production. Research Journal of Applied Sciences, Engineering and Technology. Maxwell Science Publication; 2014;**7**(20)111–122

[18] Körner O, Straten GV. Decision support for dynamic greenhouse climate control strategies. Computers and Electronics in Agriculture. 2008;**60**:18–30

[19] Berenguel M, Yebra L J, Rodríguez F. Adaptive control strategies for greenhouse temperature control. European Control Conference (ECC) IEEE. 2003. pp. 2747–2752

[20] El-Attal, A. H. Decision model for hydroponic tomato production (HYTODMOD) using utility theory (Doctoral dissertation, The Ohio State University). 1995.

[21] Short TH, Draper CM, Donnell MA. Web-based decision support system for hydroponic vegetable production. Acta Horticulturae (ISHS). 2005;**691**:867–870

[22] Shamshiri, R. Measuring optimality degrees of microclimate parameters in protected cultivation of tomato under tropical climate condition. Measurement. 2017;**106**:236–244

[23] Shamshiri, R., Che Man, H., Zakaria, A.J., Beveren, P.V., Wan Ismail, W.I. and Ahmad, D. Membership function model for defining optimality of vapor pressure deficit in closed-field cultivation of tomato. Acta Hortic. 2017:**1152**:281–290 DOI: 10.17660/ActaHortic.2017.1152.38 https://doi.org/10.17660/ActaHortic.2017.1152.38

[24] Jones, J. W., Kenig, A., & Vallejos, C. E. Reduced State–Variable Tomato Growth Model. Transactions of the ASAE. 1999;**42**(1):255–265 Doi: 10.13031/2013.13203

[25] Shamshiri R, Ahmad DB, Wan Ismail WI, Hasfalina CM, Zakaria AJ, Yamin M. Evaluation of the reduced state-variable TOMGRO model using boundary data. In: 2016 ASABE International Meeting, no. 2454205. 2016. pp. 2–12. DOI: 10.13031/aim.20162454205

[26] Acock B, Charles-Edwards DA, Fitter DJ, Hand DW, Ludwig LJ, Wilson JW, Withers AC. The contribution of leaves from different levels within a tomato crop to canopy net photosynthesis: An experimental examination of two canopy models. Journal of Experimental Botany. 1978;**29**(111):815–827

[27] Goudriaan J, Monteith JL. Mathematical function for crop growth based on light interception and leaf area expansion. Annals of Botany. 1990;**66**:695–701

[28] Vallejos, C. E., Jones J. W., and Williams F. W. High temperature tomato experiments, Ch. II-3. In Optimal Environmental Control for Indeterminate Greenhouse Crops, eds. Seginer I., Jones J.W., Gutman P. and Vallejos C. E. BARD Research Report No. IS-1995-91RC. Haifa, Israel: Agricultural Engineering Dept., Technion. 1997.